

# Acetyltransferase p300/CBP Associated Factor (PCAF) Regulates Crosstalk-Dependent Acetylation of Histone H3 by Distal Site Recognition

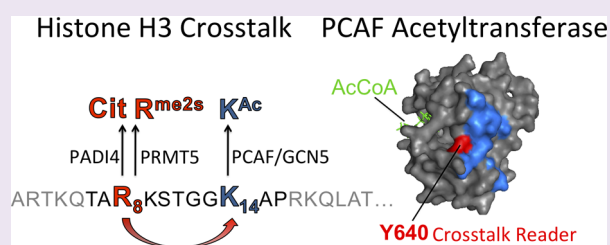
James R. Kornacki,<sup>†</sup> Andreea D. Stuparu,<sup>‡</sup> and Milan Mrksich<sup>\*,†</sup>

<sup>†</sup> Department of Biomedical Engineering, Department of Cell & Molecular Biology, and Department of Chemistry, Northwestern University, Evanston, Illinois 60208, United States

<sup>‡</sup> Department of Chemistry University of Chicago, Chicago, Illinois 60637, United States

## Supporting Information

**ABSTRACT:** Epigenetic regulation is directed, in part, by the correlated placement of histone post-translational modifications, but the mechanisms controlling correlated modifications are incompletely understood. Correlations arise from crosstalk among modifications and are frequently attributed to protein–protein interactions that recruit enzymes to existing histone modifications. Here we report the use of a peptide array to discover acetyltransferase-mediated crosstalks. We show that p300/CBP associated factor (PCAF)/GCN5 activity depends on the presence of a distal arginine residue of its histone H3 substrate. Modifications to H3 Arg8 decrease PCAF acetylation of H3 Lys14, and kinetic data indicate that arginine citrullination has the strongest effect in decreasing acetylation. Mutagenesis experiments demonstrate that PCAF specifically interprets H3 Arg8 modifications through interaction with residue Tyr640 on the surface of its catalytic domain, and this interaction regulates Lys14 acetylation by substrate discrimination. PCAF discriminates modified peptides as well as semisynthetic proteins and reconstituted nucleosomes bearing Arg8 modifications. Together, this work describes a method for systematically mapping crosstalks and illustrates its application to the discovery and elucidation of novel PCAF crosstalks.



Histone proteins are subject to a broad array of post-translational modifications that regulate gene expression, replication, and repair.<sup>1,2</sup> These modifications include acetylation, methylation, and phosphorylation, and their presence or absence at multiple sites generates staggering complexity in histone structure and function. Post-translational modification (PTM) of histone H3, for example, can theoretically generate over ten million distinct forms, and systems-level studies have catalogued a fraction of these. They reveal that distinct PTMs are generally correlated within observed histone states;<sup>3–5</sup> however, the mechanisms by which cells install and maintain these correlated modifications are much less clear. For example, many of the enzymes that modify histones lack specificity for individual sites and in many cases are localized to their substrates through interactions of adaptor domains. In this way, the action of such enzymes on their substrates generally depends on the presence or absence of other histone PTMs. A complete understanding of these indirect relationships between enzyme expression and histone modification is important for understanding regulation in the cell and in the development of drugs for so-called “epigenetic targets”. In this paper, we employ a biochip-based strategy for identifying post-translational modifications that regulate the actions of histone modifying enzymes, and we show specifically that acetylation of H3 Lys14 by the lysine acetyltransferase p300/CBP

associated factor (PCAF) is inhibited by methylation or deimination of the distal residue H3 Arg8.

This report is the first to identify a mechanism of crosstalk between methylation/deimination and acetylation on the histone. Significant earlier work has identified several examples of crosstalk where the presence or absence of a modification enhances or represses another modification on the same histone (*in cis*) or a different histone (*in trans*).<sup>6,7</sup> For example, Allis and co-workers discovered that H2B ubiquitination is a master switch of gene silencing through its effects on H3 methylation.<sup>8</sup> Oliviero and co-workers reported that phosphorylation of H3 Ser10 induces the acetylation of H4 Lys16 and directs gene activation, revealing the downstream regulatory impact of a single crosstalk activity.<sup>9</sup> The discovery of such crosstalks usually relies on a pair of antibodies to isolate histones having a first modification and to probe for the presence of a second modification, but the development of antibodies having specificity for each of the relevant modifications is challenging. In the present work, we use a combination of mass spectrometry and a peptide array, the

**Special Issue:** Post-Translational Modifications

**Received:** June 6, 2014

**Accepted:** September 9, 2014

**Published:** September 9, 2014

SAMDI method, to efficiently identify an example of crosstalk at the biochemical level where the ability of an enzyme to modify a histone sequence depends on modifications to distal residues.

We compared the acetylation of a peptide library representing mutants of the H3 Lys14 site by the acetyltransferases (KATs) PCAF and GCN5. Using this positional scanning approach, we found that the enzymes interact with Arg8 and that modification of this residue, either by methylation or deimination, significantly reduces acetylation of Lys14. Kinetic analyses confirmed the extent to which various Arg8 modifications fine-tune PCAF activity at Lys14, and we used high-resolution mass spectrometry to quantify this effect on semisynthetic H3 protein substrates and reconstituted nucleosomes. We also prepared a series of PCAF mutants and found that residue Tyr640 is necessary for recognition of Arg8 in the substrate. Together, this work provides mechanistic support for a novel *in cis* crosstalk between Arg8 methylation/deimination and Lys14 acetylation, and it also introduces a systematic and label-free strategy for identifying crosstalks that regulate the modification of histone substrates.

## RESULTS AND DISCUSSION

**PCAF-Mediated Acetylation of H3 Fragment.** PCAF is an acetyltransferase that uses the cofactor acetyl coenzyme A (AcCoA) to acetylate lysine 14 of histone 3 (H3 Lys14).<sup>10</sup> We prepared a peptide representing residues 6–16 of H3 (TARK<sub>9</sub><sup>Ac</sup>STGGK<sub>14</sub>APC), which includes the Lys14 acetylation site. The Lys9 residue in the peptide was synthetically acetylated in order to eliminate the possibility for enzymatic acetylation at that site, and the terminal cysteine residue was included for immobilization to a self-assembled monolayer. We prepared a monolayer presenting maleimide groups at a density of 10% against a background of tri(ethylene glycol) groups. The former are used to immobilize cysteine-terminated peptides, and the latter prevent the nonspecific adsorption of protein to the monolayer. The monolayer is well suited for analysis by matrix-assisted laser desorption-ionization mass spectrometry to reveal the masses of the peptide–alkanethiolate conjugates and therefore can identify products of enzyme-mediated reactions and the yields in which these products are formed. Further, the SAMDI mass spectrometry method is compatible with the analysis of peptide arrays and was used in the present work to profile acetyltransferase activities across 73 distinct substrates.<sup>11–13</sup>

To assay PCAF activity, we applied a solution containing the enzyme and cofactor (1  $\mu$ M PCAF, 100  $\mu$ M AcCoA, 50 mM Tris pH 8.0, 0.1 mM EDTA) to a monolayer presenting the H3 peptide substrate. The reaction was incubated for 1 h. The monolayer was then rinsed, treated with matrix, and analyzed by mass spectrometry (Figure 1). The SAMDI spectrum of the original monolayer has a peak at  $m/z = 2110$  that corresponds to the peptide–alkanethiolate conjugate. Following the reaction, a spectrum revealed a new peak at  $m/z = 2152$  that corresponds to the acetylated form of the peptide. Integration of peak areas showed that acetylation proceeded in 70% yield.

**Distal Sequence Scanning.** We designed a library of peptide substrates that could be used to identify whether PCAF interacts with H3 residues distal to the Lys14 acetylation site. The library included the following 73 peptides that represent the wild-type sequence and each possible mutant at positions 7–10 of histone H3: TX<sub>7</sub>RK<sup>Ac</sup>STGGK<sub>14</sub>APC, TAX<sub>8</sub>K<sup>Ac</sup>STGGK<sub>14</sub>APC, TARX<sub>9</sub>STGGK<sub>14</sub>APC, and TAR-

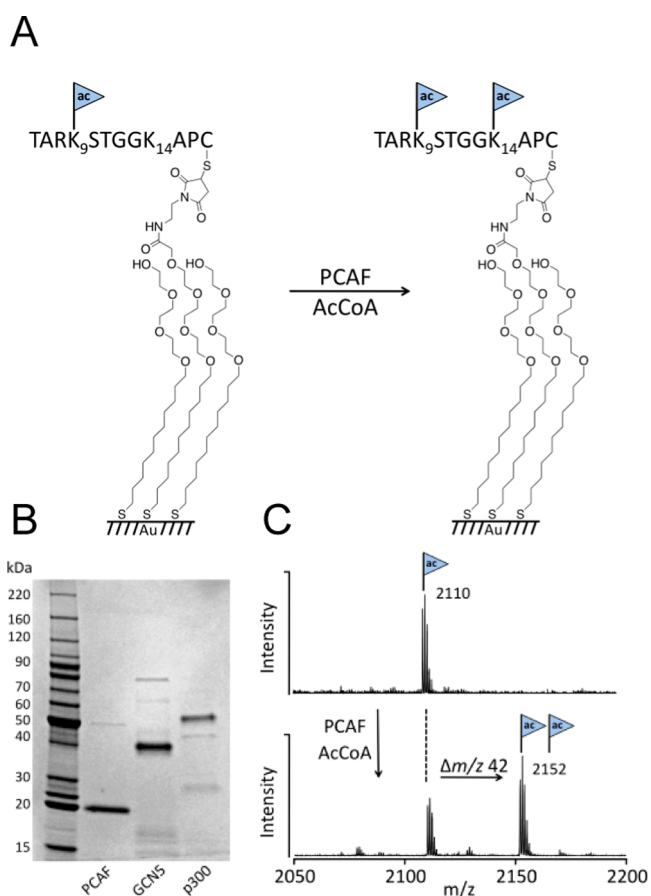


**Figure 1.** Schematic of the SAMDI acetylation assay. (A) Self-assembled monolayers presenting maleimide against a background of tri(ethylene glycol) are appended with the H3 substrate TARK<sub>9</sub><sup>Ac</sup>STGGK<sub>14</sub>APC and treated with PCAF/AcCoA to generate the enzymatically acetylated product. (B) SDS-PAGE of expressed acetyltransferases PCAF, GCN5, and p300. (C) A SAMDI spectrum of the initial monolayer has a peak at  $m/z = 2110$  corresponding to the peptide–alkylthiolate conjugate. Following treatment with PCAF, the acetylated product peptide is observed at  $m/z = 2152$ .

K<sup>Ac</sup>X<sub>10</sub>TGGK<sub>14</sub>APC, where X is substituted with any of the natural amino acids except for cysteine. Again, lysine 9 was synthetically acetylated to restrict enzymatic acetylation to lysine 14. The peptides were immobilized on an array of monolayers arranged in standard 384-well format as recently described.<sup>13</sup> The reaction conditions were adjusted to give an approximate 85% conversion on the wild-type sequence. Reaction mixtures were automatically dispensed to the array and incubated for 1 h. Next, the monolayers were rinsed and analyzed by SAMDI mass spectrometry to determine the extent of reaction of each peptide, which is shown in a bar graph plot (Figure 2). These data reveal a striking dependence on the Arg8 residue for acetylation at Lys14 by PCAF. Substitution of this arginine with either histidine or lysine gives weak activity, while peptides having other residues at this position are not acetylated at all. By contrast, PCAF is remarkably tolerant to mutations at positions 7, 9, and 10, with only K9ac  $\rightarrow$  D and S10  $\rightarrow$  G/P showing at least a 3-fold reduction in acetylation of Lys14. Hence, PCAF recognizes the Arg8 residue of its substrate.

To assess whether distal site dependence might be a common feature of KATs, we tested the acetyltransferase GCN5 and p300. GCN5 is structurally similar to PCAF, while

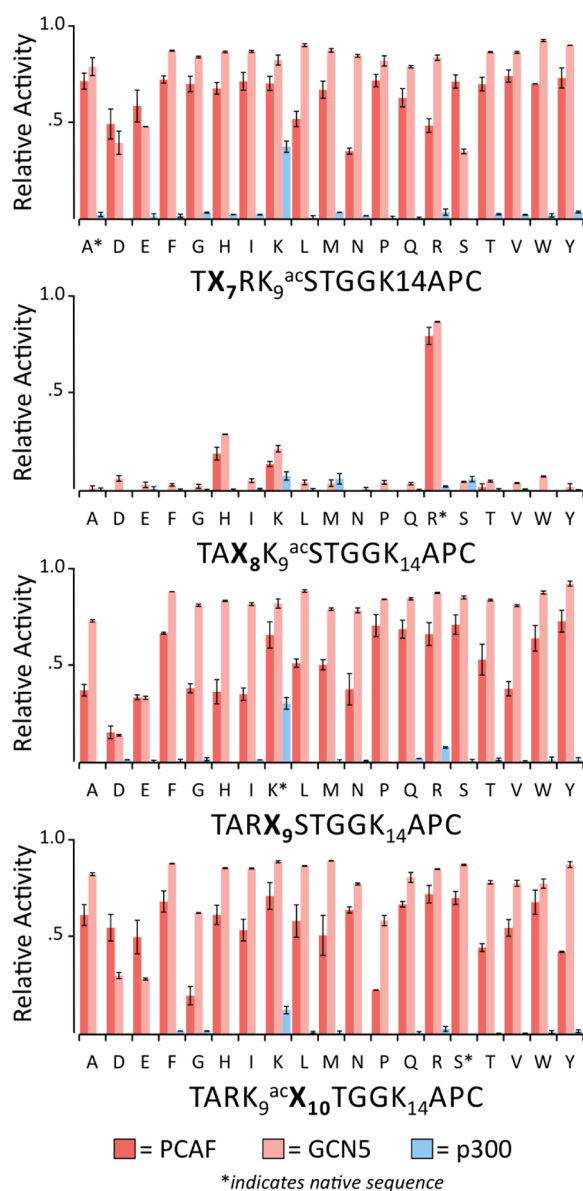


**Figure 2.** Distal sequence scanning assay for selected KATs on H3 peptides mutated at positions 7–10 by SAMDI mass spectrometry. Bars indicate relative acetylation  $\pm$  SD ( $n = 3$ ) for each substrate following treatment with PCAF, GCN5, or p300. The X position in each substrate set is substituted with all natural amino acids, except cysteine.

p300 is structurally distinct. These KATs also prefer different histone and non-histone substrates.<sup>14,15</sup> p300 was weakly active at Lys14 and did not reveal a strict dependence on distal sequence variation. Instead, it preferred substrates that included a lysine mutation, consistent with reports that p300 prefers substrates with a distal lysine residue.<sup>15,16</sup> GCN5 is structurally homologous to PCAF and shared the same requirement for Arg8. It was similarly tolerant to substrate mutations at positions 7, 9, and 10.

**PCAF Kinetics on Arg8-Modified Substrates.** Known PTMs to H3 Arg8 include methylation<sup>17</sup> and deimination,<sup>18</sup> and we therefore determined whether those modifications to the peptide substrates had an impact on acetylation by PCAF. We synthesized peptides having each of the four possible modified forms, monomethyl ( $R_{me}$ ), symmetric dimethyl

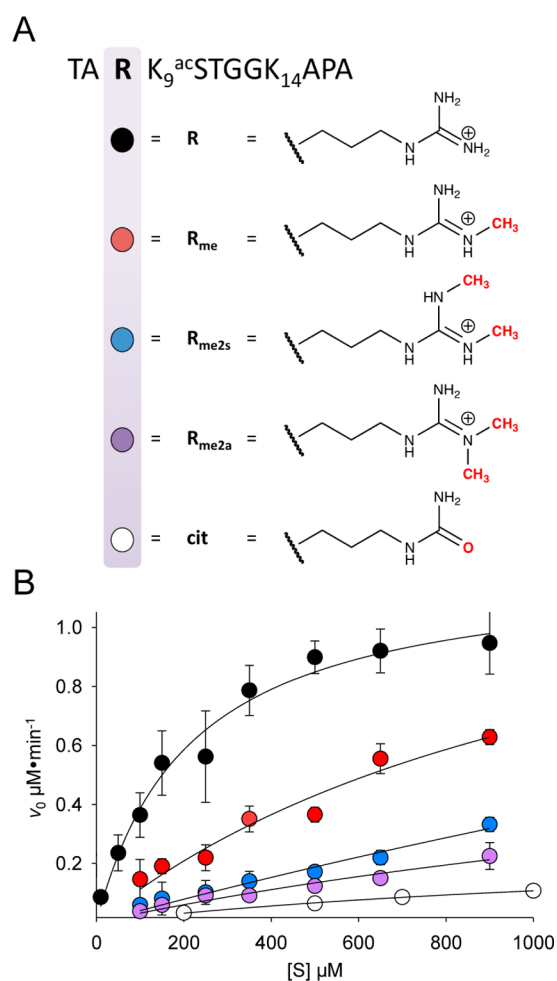


**Figure 3.** Arginine PTMs and kinetic data for PCAF on Arg8-modified H3 peptides. (A) Structures of the arginine side chain (R) with modifications including methyl ( $R_{me}$ ), symmetric dimethyl ( $R_{me2s}$ ), asymmetric dimethyl ( $R_{me2a}$ ), and citrulline (cit) forms. (B) Kinetic plot of PCAF on modified H3 substrates by a solution-phase kinetic assay. Substrate concentration was varied while holding PCAF and AcCoA concentrations constant. Each spot represents an average of initial reaction velocities performed in triplicate.

( $R_{me2s}$ ), asymmetric dimethyl ( $R_{me2a}$ ), and the deiminated form having the amino acid citrulline (cit), and we characterized their activity toward PCAF (Figure 3). Determining Michaelis–Menten kinetics in cases where the enzyme is soluble and the substrate is immobilized can be challenging.<sup>19</sup> For this reason, we employed a solution-phase spectrophotometric assay developed by Denu and co-workers.<sup>20</sup> We determined kinetic profiles for the reaction across varying substrate concentrations (10–1300  $\mu\text{M}$ ), while maintaining PCAF and AcCoA concentration at 1 and 100  $\mu\text{M}$ , respectively. The initial velocities displayed a stepwise increase in  $K_M$  as the native Arg8 was mutated to  $R_{me}$ ,  $R_{me2s}$ ,  $R_{me2a}$ , and finally cit. Generally,  $k_{cat}$  remained constant between the mutants, apart from the citrulline mutant, which was near the limit of resolution. The dimethyl and citrullinated peptides had a 10-fold reduction in catalytic efficiency ( $k_{cat}/K_M$ ) owing primarily to an increase in  $K_M$  (Table 1).

**Histone and Nucleosome Substrates.** We next verified that our finding of an Arg8-dependent PCAF activity was not an artifact stemming from the use of a peptide substrate but also operated for protein and nucleosome substrates. We used

**Table 1. Summary of Michaelis–Menten Constants for PCAF**

substrate, S	$K_M^a$ (mM)	$k_{cat}^a$ ( $\text{min}^{-1}$ )	$k_{cat}/K_M$ ( $\text{M}^{-1} \text{min}^{-1}$ )
R	$0.21 \pm 0.04$	$1.2 \pm 0.1$	5700
$R_{me}$	$1.2 \pm 0.5$	$1.5 \pm 0.5$	1260
$R_{me2s}$	$2.9 \pm 1.3$	$1.3 \pm 0.5$	450
$R_{me2a}$	$2.5 \pm 0.7$	$0.8 \pm 0.5$	320
Cit	$3.7 \pm 0.9$	$0.5 \pm 0.2$	140

<sup>a</sup>Reported values are an average  $\pm$  SEM of three independent experiments.

native chemical ligation to prepare full-length H3 proteins that had modified forms of Arg8.<sup>21</sup> We synthesized appropriate peptide thioesters representing residues 1–24 of H3 containing the desired Arg8 modification and performed ligation reactions with a recombinant truncated H3 protein bearing an N-terminal cysteine in place of the native alanine residue at position 25. For these experiments, Lys9 was not synthetically acetylated. Reactions were performed by adding the protein substrate to a solution containing PCAF (20 nM, 100  $\mu$ M AcCoA, 50 mM Tris, pH 8.0, 0.1 mM EDTA), allowing the reaction to proceed for 10 min at 30  $^{\circ}$ C, and terminating by heating to 100  $^{\circ}$ C.

To assess the extent of enzymatic acetylation at Lys14, we employed high-resolution mass spectrometry (MS) as described by Smith and co-workers.<sup>22</sup> Briefly, quenched reactions were treated with deuterated acetic anhydride to isotopically label all lysine amino groups that had not been enzymatically acetylated in the reaction. Subsequent trypsin digestion generated differentially labeled peptide precursors that were chemically equivalent and therefore not susceptible to differences in ionization efficiency despite variation in the extent of enzymatic modification across samples. We focused on the peptide precursor containing Lys14 and quantified the degree of acetylation by comparing the abundance of the enzymatically acetylated species to its artificially labeled counterpart at +3 Da. The precursor containing Lys14 also contained Lys9. In cases where Arg8 was dimethylated ( $R_{me2a}$ ,  $R_{me2s}$ ) or deiminated (cit), the peptide precursor also contained Lys4 since trypsin does not cleave after these modifications. To resolve the site(s) of enzymatic acetylation and to confirm the identity of the doubly charged precursor, all monoacetylated species were independently isolated for collision-induced dissociation (CID).

The unmodified, chemically ligated H3 substrate (R) yielded approximately 60% acetylation at Lys14 by PCAF as evidenced by the relative total ion current (TIC) of the enzymatically acetylated species ( $m/z = 494.78$ ) versus the fully labeled species ( $m/z = 496.29$ ). Fragmentation of the enzymatically acetylated species unambiguously showed activity at Lys14 and not Lys9. The most significant reduction in acetylation was observed for the citrullinated substrate, which had a 3-fold decrease in activity, although some PCAF acetylation of Lys4 contributed to this measurement. Precursor peptides from the dimethylated ( $R_{me2a}$ ,  $R_{me2s}$ ) and deiminated (cit) substrates also indicated partial PCAF acetylation of Lys4, but such modification accounted for less than 10% of the enzymatic activity as indicated by the CID spectra (Supplementary Figure 1, Supporting Information). Despite the contribution of Lys4 acetylation to the measured activity, a decrease in acetylation was observed across the Arg8-modified forms (Figure 4, Table 2). The trend is consistent with that observed using the peptide

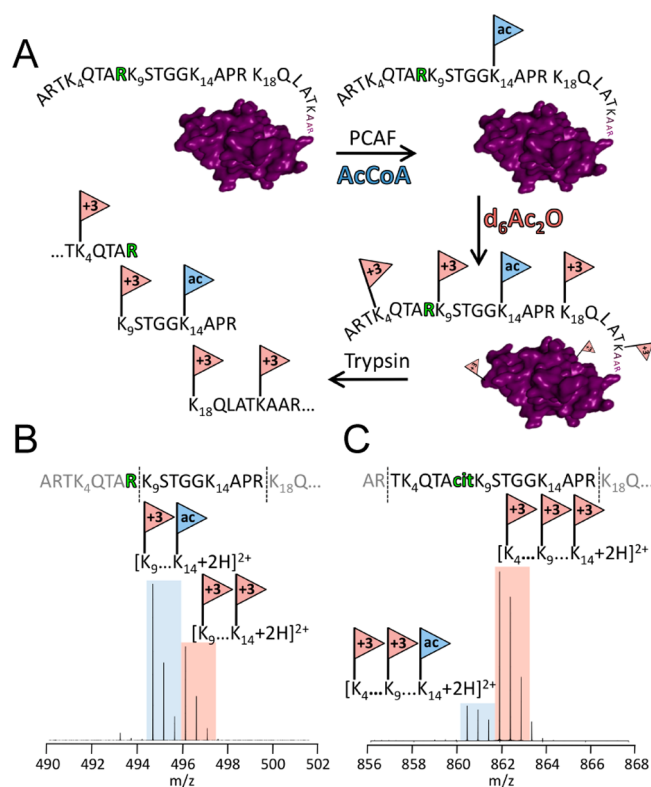


**Figure 4.** Quantitation of Lys14 acetylation by PCAF on semisynthetic protein substrates by bottom-up proteomics. (A) Experimental protocol: histone protein is first acetylated by PCAF, then quenched and treated with deuterated acetic anhydride to attach a +3 acetyl label to any free lysine residues. Digestion with trypsin yields chemically equivalent peptides for analysis by high-resolution LC-MS. (B) MS1 spectrum of the labeled precursor containing Lys14 from the unmodified semisynthetic substrate (R) indicating approximately 60% relative acetylation. (C) MS1 spectrum of the labeled precursor containing Lys14 from the citrullinated semisynthetic substrate (cit) indicating approximately 20% relative acetylation. Dashed lines denote trypsin cleavage sites. Experiments were performed in triplicate.

**Table 2. Relative Extent of Lys14 Acetylation by PCAF on Modified H3 Proteins**

histone H3 proteins	relative Lys14 acetylation <sup>a</sup> (%)
commercial standard	$79 \pm 12$
unmodified (R)	$58 \pm 5$
monomethyl ( $R_{me}$ )	$46 \pm 13$
asymmetric dimethyl ( $R_{me2a}$ )	$32 \pm 4^b$
symmetric dimethyl ( $R_{me2s}$ )	$22 \pm 3^b$
citrulline (cit)	$21 \pm 1^b$

<sup>a</sup>Reported values are an average  $\pm$  SD of three independent experiments. <sup>b</sup>Measurement includes contribution from Lys4 acetylation.

substrates but less pronounced in that the most disruptive modifications,  $R_{me2s}$  and cit, yielded a 3-fold reduction in acetylation versus an approximate 10-fold reduction observed for peptides. We tested a commercially available recombinant H3 protein standard and found approximately 80% Lys14 acetylation, suggesting that semisynthetic substrates are not perfect biological mimics of endogenous H3.

Because H3 is found almost exclusively within chromatin, we reconstituted nucleosomal particles that were modified at H3 Arg8. We used a commercially available H3 that was



dimethylated at Arg8 (H3R8me2a) and assembled a histone octamer according to the method of Luger.<sup>23</sup> Nucleosome core particles (NCPs) were prepared in the presence of a standard DNA sequence amplicon by a gradual reduction in ionic strength. Confirmation of nucleosome formation was visualized by a gel-shift assay on native polyacrylamide gels stained for DNA. NCPs were assayed and analyzed by mass spectrometry according to the preceding protocol. Relative PCAF acetylation of Lys14 was determined to be 62% for the unmodified NCP and 19% for the H3R8me2a NCP.

**PCAF Mutagenesis.** We reasoned that this crosstalk is mediated by an interaction of the Arg8 residue with PCAF by way of a site on the surface of the enzyme. To examine this possibility, we generated several PCAF mutants that substituted residues near the enzyme active site with an alanine. We used structural data for PCAF and the homologous GCN5 to target mutations on the surface of the protein near the peptide binding cleft.<sup>24–27</sup> We site-specifically mutated amino acids situated in the catalytically important  $\alpha 2$  helix region (residues 530–540) and the  $\alpha 5$ – $\beta 6$  loop (residues 535–644), which are known to rearrange during substrate binding (Figure 5). Following verification by SDS-PAGE and DNA sequencing, each mutant was tested for its ability to preserve or impair crosstalk.

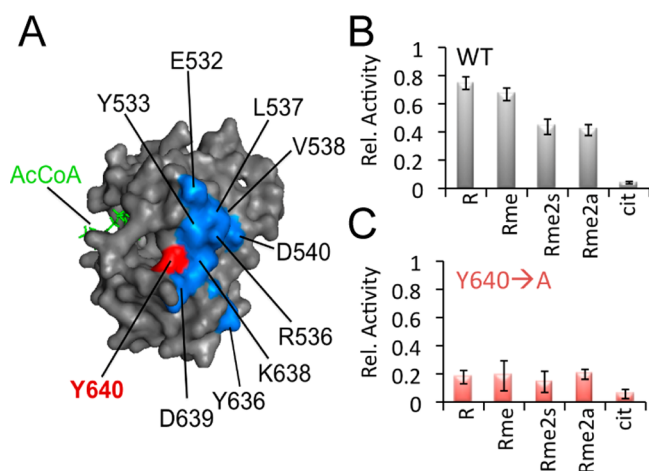


**Figure 5.** Mutation of Tyr640 eliminates crosstalk capability. (A) PCAF illustration highlighting the amino acids mutated to alanine. PCAF H3 Lys14 acetylation activity by SAMDI on Arg8-modified peptides for wild-type PCAF (B) and Y640A mutant (C). Bars indicate relative acetylation  $\pm$  SD ( $n = 3$ ).

We assayed each mutant by SAMDI-MS against a panel of peptides having R, R<sub>me</sub>, R<sub>me2s</sub>, R<sub>me2a</sub>, or cit at position 8. Most of the mutants displayed a trend in activity on these substrates that was similar to wild-type, suggesting that their respective residues do not participate in the putative interaction with Arg8. One mutant, Y640A, had a reduced, but near-constant, activity on each of the substrates (Figure 5). Hence, this mutant uncoupled acetylation of Lys14 from recognition of Arg8, suggesting that the tyrosine residue mediates the interaction with Arg8, perhaps using a cation– $\pi$  interaction.<sup>28</sup> Tyr244 in yGCN5 is analogous to PCAF Tyr640 and is also located within the peptide binding cleft distal to the active site. Interestingly, this single point mutant has been found to decrease acetylation activity *in vivo*.<sup>27</sup> Despite the slight structural differences between GCN5 and PCAF, we believe

that our results extend the importance of this residue as a substrate reader required for crosstalk functionality.

The dependence of PCAF-mediated acetylation of H3 Lys14 on the Arg8 residue establishes a novel crosstalk between these sites. Modifications at Arg8 impaired PCAF-mediated acetylation of Lys14 with dimethyl arginine and citrulline proving most significant. Kinetic analyses of Arg8-modified peptides verified a stepwise reduction in acetylation from the native substrate to the monomethylated, dimethylated, and deiminated forms. We also observed this crosstalk on full-length H3 protein substrates prepared semisynthetically and on reconstituted nucleosomes, although the observed effect was less pronounced. In these instances, the availability of additional sequence contacts may have compensated for the disrupted interaction with PCAF Tyr640 caused by Arg8 modifications, which our kinetic studies revealed to affect peptide affinity.

Studies using peptide substrates provide a convenient platform for investigating biochemical properties of enzymes but often do so at the expense of true biological context. Our experiments on the histone H3 positional mutant peptide library allowed the facile determination of Arg8 dependence for PCAF/GCN5 when arranged in array format for automated handling and analysis. The more challenging characterization on semisynthetic protein substrates and reconstituted nucleosomes revealed that our peptide-level work reliably approximated the solution-phase *in vitro* outcomes. Still, the mechanism of PCAF regulation by distal site recognition remains to be verified *in vivo* in order to truly appreciate the biological importance of this crosstalk and the many other crosstalks that support correlated histone states.

New examples of crosstalk continue to redefine the epigenetic landscape, but in most cases, these examples do not include a biochemical rationale. In those cases that do, the mechanistic insight generally focuses on adaptor-mediated recognition rather than substrate discrimination by catalytic domains.<sup>29,30</sup> Our mutagenesis experiments revealed that Tyr640 of the PCAF catalytic domain participates in recognizing the methylation/deimination state of Arg8 via a distal site interaction. Biochemical studies of the PCAF paralogue GCN5 by Marmorstein and Poux hypothesized that residues N-terminal to H3 Lys14 are particularly important to substrate affinity,<sup>14</sup> and our data support this notion of distal site dependence. Mutagenesis experiments by Allis and co-workers found several GCN5 surface residues critical to catalytic function *in vivo*, including Tyr244, the analogue of PCAF Tyr640.<sup>27</sup> Hence, the catalytic importance of these residues may then derive from their role as crosstalk mediators, but this association needs to be studied further.

This and related forms of crosstalk may underlie the correlations of PTMs that are often observed on histones. Kelleher and co-workers, for example, noted such correlations in HeLa nuclei arising from the placement of methyl and acetyl marks on histone H4.<sup>31</sup> Correlations of modifications at Arg8 and Lys14 have not been reported, but this work illustrates a mechanism by which PCAF could maintain a correlated state via these two residues. Given the overwhelming combinatorial complexity of theoretical histone modifications, we believe it reasonable that histone modifiers participate in crosstalk to engage a more tractable number of states.

Known H3 Arg8 post-translational modifications include symmetric dimethylation by protein arginine methyltransferase 5 (PRMT5)<sup>17</sup> and deimination to citrulline by protein arginine deiminase 4 (PAD4),<sup>18</sup> but their impact on Lys14 is not yet

clear. Genome-wide epigenetic profiles in mice have linked Lys14 acetylation to a subset of inactive promoters “poised” for transcriptional activation.<sup>32</sup> The repressive link between Arg8 modifications and PCAF-mediated Lys14 acetylation may then predict a repressive function overall, but such speculation awaits *in vivo* demonstration.

Whether modification states codify defined regulatory signatures remains to be firmly established. Still, aberrant modifications are observed in diseased cells, and the enzymes that regulate histone modification have become important targets in drug development programs. For example, many cancers are associated with hypoacetylation mediated possibly by the overexpression of deacetylases.<sup>33,34</sup> The drugs vorinostat and romidepsin for the treatment of cutaneous T-cell lymphoma are thought to work by boosting acetylation.<sup>35,36</sup> Our work suggests the interesting possibility that inhibition of Arg8 modifiers could also be used to increase acetylation and gives additional targets to explore. Decoding crosstalks is therefore requisite to the expansion of epigenetic targeting.

Finally, our work provides a systematic method for identifying relationships in enzyme activities that may provide for crosstalk on the histone tails. The label-free positional scanning assay combines peptide arrays with SAMDI mass spectrometry for the identification of substrate sequence dependence. When distal sequence residues harbor PTM potential, the assay becomes a crosstalk discovery tool. Our focus on histone H3 led to the discovery and elucidation of a novel PCAF-mediated crosstalk between Arg8 methylation/deimination and Lys14 acetylation. The assay is not, however, limited to acetyltransferases. Extending the method to other histone and non-histone proteins ought to reveal several new associations between enzymes and modifications otherwise considered distinct.

## METHODS

**General.** Unless specified otherwise, laboratory chemicals and reagents were purchased from Sigma-Aldrich and used without additional purification. Peptide synthesis reagents, including Fmoc amino acids and Rink-amide resin, were purchased from Anaspec. Selectively methylated Fmoc-arginine amino acids and H-Ala-sulfamylbutyryl NovaSyn TG resin are products of Novabiochem (EMD Millipore). Plasmids containing human PCAF and histone H3.3 were purchased from ATCC, and remaining molecular biology materials were purchased from Invitrogen. Oligonucleotide primers were from Integrated DNA Technologies. Restriction endonucleases, recombinant human histones, and control DNA were purchased from New England Biolabs. Histone H3R8me2a protein was purchased from ActiveMotif. Spectrophotometric data were collected on a DU-640 spectrophotometer (Beckman Coulter) unless indicated otherwise. Matrix-assisted laser desorption/ionization (MALDI)-time of flight (TOF) and self-assembled monolayers with matrix-assisted laser desorption-ionization (SAMDI)-TOF mass spectrometry were performed on a 4800 MALDI TOF/TOF mass spectrometer (Applied Biosystems) by manual and automated protocols. High-resolution proteomic data were obtained on an Orbitrap Velos mass spectrometer equipped with a nanoflow HPLC (Thermo Scientific). Gel filtration was performed on an ÄKTA FPLC. All experiments were performed in triplicate.

**Protein Expression and Purification.** Recombinant plasmids (pTriEx-3, Novagen EMD Millipore) harboring genes for human PCAF catalytic domain (aa 492–658), full-length human GCN5, or human p300 catalytic domain (aa 1284–1673) were confirmed via bidirectional DNA sequencing and expressed in *Escherichia coli* [BL21(DE3)] (Invitrogen) by isopropyl- $\beta$ -D-galactopyranoside (IPTG) induction (0.5  $\mu$ M final) for 4 h at 37 °C after reaching an OD of 0.4–0.6. After lysis by sonication in the presence of protease

inhibitors (Roche), the soluble 6 $\times$  His-tagged proteins were purified on a prepared IMAC column containing Co<sup>2+</sup> HisPur affinity resin (Thermo) and eluted across a stepwise imidazole gradient (10–150 mM) in 50 mM Tris-HCl, pH 7.5, 200 mM NaCl, 5% glycerol, and 5 mM  $\beta$ -mercaptoethanol. Pure fractions were determined by SDS-PAGE on a 4–12% polyacrylamide gel (Lonza), concentrated with centrifugal filters (Millipore), dialyzed against storage buffer (50 mM Tris-HCl, pH 8.0, 10% glycerol, 0.1 mM EDTA), flash frozen, and stored at –80 °C. Protein concentration was determined on a NanoDrop spectrophotometer (Thermo Scientific) using calculated extinction coefficients (PCAF  $\epsilon_{280} = 20525 \text{ M}^{-1} \text{ cm}^{-1}$ , GCN5  $\epsilon_{280} = 53290 \text{ M}^{-1} \text{ cm}^{-1}$ , p300  $\epsilon_{280} = 42860 \text{ M}^{-1} \text{ cm}^{-1}$ ). Expression was confirmed by SDS-PAGE (Figure 1).

Truncated human histone H3.3 protein was expressed in BL21-(DE3) harboring pET21a(+) according to standard protocols.<sup>37,38</sup> Briefly, the gene encoding truncated H3 (amino acids 26–135) was amplified from the plasmid containing full-length human histone H3.3 with a forward primer designating an *Nde*I site, a start codon, codons establishing a Factor Xa protease cleavage site (amino acids IEGR), and a codon for an N-terminal cysteine residue (5'-ACTG CAT ATG ATC GAA GGT CGT TGT AGG AAA AGC GCT CCC-3'), while the reverse primer encoded an *Xho*I site (5'-ACTG CTC GAG AGC TCT CTC TCC CCG TAT CCG G-3'). Plasmids were maintained and propagated in *E. coli* (DH5 $\alpha$ , Novagen), and DNA sequencing validated the identity of the expression plasmid. Following induction by 0.2  $\mu$ M IPTG (final) for 2 h at 37 °C, the 6 $\times$  His-tagged protein was purified from inclusion bodies with Co<sup>2+</sup> affinity chromatography as described above. Fractions were dialyzed against three changes of 5 mM dithiothreitol (DTT), analyzed by SDS-PAGE on a 15% polyacrylamide gel (Lonza) and by MALDI-TOF mass spectrometry (linear midmass positive mode,  $m/z = 14335$ ). Protein concentration was determined spectrophotometrically ( $\epsilon_{280} = 4470 \text{ M}^{-1} \text{ cm}^{-1}$ ), and the protein was flash frozen and stored at –80 °C.

**Peptide Synthesis.** Solid-phase peptide synthesis was performed on Rink-amide lanterns (Mimotopes) housed in 96-well filter plates. Deprotection of N-terminal fluorenylmethyloxycarbonyl (Fmoc) protecting groups was achieved with 20% piperidine in dimethylformamide (DMF) at RT after 15 min. Lanterns were filtered and rinsed 5 times with DMF on a multiscreen vacuum manifold (Millipore). DMF solutions containing 15 mol equiv of Fmoc-amino acids, benzotriazol-1-yl-oxypyrrolidinophosphonium hexafluorophosphate (PyBOP), and 30 mol equiv of 4-methylmorpholine were applied to each lantern and coupling proceeded for 30 min. Coupling reactions beyond the sixth terminal position were performed twice. Following deprotection of the ultimate residue, the N-terminus was acetylated with 10% acetic anhydride in DMF for 15 min. Peptides were cleaved and deprotected simultaneously in 95% trifluoroacetic acid (TFA), 2.5% triethylsilane (TES), and 2.5% water for 2 h. TFA was evaporated under a stream of nitrogen, and the peptides were resuspended in deionized ultrafiltered (DIUF) water, analyzed by MALDI-TOF MS in positive reflector mode (20 kV accelerating voltage, 400 laser shots per spot), and lyophilized. After resuspension in 0.1% TFA in water, peptides were stored at –20 °C.

Peptides required for kinetic studies were synthesized according to the outlined procedure with a few modifications. Rink-amide 4-methylbenzhydramine (MBHA) resin was used in place of lanterns and treated with 4 mol equiv of Fmoc-amino acid/PyBOP and 8 mol equiv of N-methylmorpholine (NMM). Purification was achieved by reverse phase HPLC (Waters) along a linear gradient from 0% solvent A (0.1% aqueous TFA) to 100% solvent B (75% acetonitrile, 25% water, 0.1% TFA) for 65 min with a C18 semiprep column (Macherey–Nagel).

Peptide thioesters were prepared similarly, but required sulfamylbutyryl resin, and we opted for one preloaded with alanine. The nascent chain was terminated with Boc-alanine. Activation, cleavage, and deprotection were performed according to standard methods.<sup>39</sup>

**Acetyltransferase Assays by SAMDI Mass Spectrometry.** Self-assembled monolayers of mixed alkyl thiolates on gold were prepared and analyzed according to previously reported methods.<sup>13</sup> Briefly, pH-neutral solutions of cysteine-terminated peptides were incubated for 1

h atop monolayers presenting maleimide-terminated alkyl thiolates at a density of 10% against an inert background of tri(ethylene glycol) and rinsed with ethanol. Immobilized substrates for enzyme-optimized controls were as follows: TARK<sup>Ac</sup>STGGKAPC for PCAF/GCN5 and SGRGK<sup>Ac</sup>GGRGLC for p300. Enzymatic reactions in KAT buffer (100  $\mu$ M AcCoA, 50 mM Tris, pH 8.0, 0.1 mM EDTA) were initiated by the addition of enzyme (1  $\mu$ M PCAF, 250 nM GCN5, or 250 nM p300) to the preimmobilized substrate by the aid of a Multidrop Combi liquid handler (Thermo), which dispensed 2  $\mu$ L droplets per monolayer spot. Plates were incubated at 30 °C (1 h for PCAF and p300, 3 h for GCN5) and rinsed extensively with water and ethanol. Minimal matrix (30 mg mL<sup>-1</sup> 2,4,6-trihydroxyacetophenone in acetone) was applied before MS analysis. Enzymatic yields were quantified by inputting the areas under the curve (AUCs) for the acetylated product peak and the substrate peak into the following formula:  $AUC_{Product}/(AUC_{Product} + AUC_{Substrate})$ . AUCs were calculated by Applied Biosystems Data Explorer software after Gaussian smoothing and baseline subtraction. MS/MS was performed by collision-induced dissociation (CID) of the monoacetylated, protonated precursor after desorption directly from the monolayer surface. CID was performed at 2 keV collision energy with air as the collision gas. Thirty spectra were acquired and ensemble averaged.

**Kinetics.** First-order kinetic parameters were established for recombinant PCAF on methylated/citrullinated histone H3 substrates by a coupled enzymatic assay developed by Denu and co-workers.<sup>20</sup> Substrate concentration was varied (10  $\mu$ M to 1.3 mM) for each triplicate data point, while AcCoA and PCAF concentrations were held constant at 100 and 1  $\mu$ M, respectively. Reactions were initiated by the addition of PCAF and maintained at 30 °C. Kinetic traces proceeded for 30 min, and initial velocities were recorded after the trace had attained linearity. Data were plotted in Sigmaplot (Systat Software) and fitted to hyperbolic and linear (double reciprocal) kinetic functions.

**Semisynthetic Protein Engineering.** Intact histone H3.3 proteins were prepared via a native chemical ligation strategy<sup>40,41</sup> according to the protocol by Peterson and co-workers<sup>21,38</sup> with the aforementioned modifications regarding peptide thioester synthesis and truncated histone H3.3 expression. Additionally, the N-terminal cysteine of truncated histone H3.3 was exposed by Factor Xa protease (New England Biolabs) for 45 min in the prescribed buffer, quenched with 1 mM phenylmethylsulfonyl fluoride, and dialyzed to remove salts. Soluble protein was immediately purified to remove undigested and overdigested species by C4 reverse phase HPLC. Pure fractions were lyophilized and weighed. Digested protein was resuspended in ligation buffer (1% benzyl mercaptan, 1% thiophenol, 3 M guanidine-HCl, 100 mM potassium phosphate, pH 7.9) to a concentration of 2–5 mM. 1.5 mol equiv of peptide thioester was added, and the reaction tube was flushed with nitrogen. Ligation proceeded for 20 h at RT.<sup>42</sup> Full-length protein containing the desired arginine modifications was purified by FPLC (ÄKTA) on a HiTrap sulfopropyl-Sepharose high-performance ion-exchange column (GE Healthcare) using the deionized urea buffers recommended by Luger et al.<sup>37</sup> Pure protein was dialyzed extensively against 2 mM DTT, concentrated, and quantified on a NanoDrop spectrophotometer before storage at –80 °C. The entire protocol was monitored by MALDI-MS operating in linear mode.

**Designer Nucleosome Assembly.** The microscale reconstitution of nucleosome core particles with human histones and either native H3 or H3R8me2a was performed by the method of Luger and co-workers.<sup>23</sup> DNA was amplified from a 208 bp *Lytechinus variegatus* 5Sr sequence using the following PCR primers: 5'-ACTTCCAGGGATTTATAAGCCG-3' (forward), 5'-TATTCGTTGGAATTCCTCGGG-3' (reverse). DNA binding to purified octamers was achieved by gradual stepwise dilution from 2 M NaCl to 250 mM NaCl followed by dialysis into buffer (50 mM Tris, pH 8.0, 0.1 mM EDTA) and spin concentration.

**Quantification of Acetylation by Mass Spectrometry.** Semisynthetic histone H3.3 and reconstituted nucleosomes were subject to *in vitro* acetylation by PCAF.

## ■ ASSOCIATED CONTENT

### ● Supporting Information

Quantification of acetylation by mass spectrometry and supplementary methods. This material is available free of charge via the Internet at <http://pubs.acs.org>.

## ■ AUTHOR INFORMATION

### Corresponding Author

\*Milan Mrksich. E-mail: [milan.mrksich@northwestern.edu](mailto:milan.mrksich@northwestern.edu).

### Notes

The authors declare no competing financial interest.

## ■ ACKNOWLEDGMENTS

We thank the Northwestern University Proteomics Core facility for aiding the quantitative proteomics work. Research reported in this publication was supported by the National Institutes of Health under Award Number R01GM084188

## ■ REFERENCES

- (1) Jenuwein, T., and Allis, C. D. (2001) Translating the histone code. *Science* 293, 1074–1080.
- (2) Strahl, B. D., and Allis, C. D. (2000) The language of covalent histone modifications. *Nature* 403, 41–45.
- (3) Gardner, K. E., Allis, C. D., and Strahl, B. D. (2011) OPERating ON Chromatin, a Colorful Language where Context Matters. *J. Mol. Biol.* 409, 36–46.
- (4) Lee, J. S., Smith, E., and Shilatifard, A. (2010) The Language of Histone Crosstalk. *Cell* 142, 682–685.
- (5) Oliver, S. S., and Denu, J. M. (2011) Dynamic Interplay between Histone H3 Modifications and Protein Interpreters: Emerging Evidence for a “Histone Language”. *ChemBioChem* 12, 299–307.
- (6) Latham, J. A., and Dent, S. Y. R. (2007) Cross-regulation of histone modifications. *Nat. Struct. Mol. Biol.* 14, 1017–1024.
- (7) Yang, X. J., and Seto, E. (2008) Lysine acetylation: Codified crosstalk with other posttranslational modifications. *Mol. Cell* 31, 449–461.
- (8) Briggs, S. D., Xiao, T. J., Sun, Z. W., Caldwell, J. A., Shabanowitz, J., Hunt, D. F., Allis, C. D., and Strahl, B. D. (2002) Gene silencing - Trans-histone regulatory pathway in chromatin. *Nature* 418, 498–498.
- (9) Zippo, A., Serafini, R., Rocchigiani, M., Pennacchini, S., Krepelova, A., and Oliviero, S. (2009) Histone Crosstalk between H3S10ph and H4K16ac Generates a Histone Code that Mediates Transcription Elongation. *Cell* 138, 1122–1136.
- (10) Schiltz, R. L., Mizzen, C. A., Vassilev, A., Cook, R. G., Allis, C. D., and Nakatani, Y. (1999) Overlapping but distinct patterns of histone acetylation by the human coactivators p300 and PCAF within nucleosomal substrates. *J. Biol. Chem.* 274, 1189–1192.
- (11) Min, D. H., Tang, W. J., and Mrksich, M. (2004) Chemical screening by mass spectrometry to identify inhibitors of anthrax lethal factor. *Nat. Biotechnol.* 22, 717–723.
- (12) Mrksich, M., and Whitesides, G. M. (1997) Using self-assembled monolayers that present oligo(ethylene glycol) groups to control the interactions of proteins with surfaces. *ACS Symp. Ser.* 680, 361–373.
- (13) Gurard-Levin, Z. A., Scholle, M. D., Eisenberg, A. H., and Mrksich, M. (2011) High-Throughput Screening of Small Molecule Libraries using SAMDI Mass Spectrometry. *ACS Comb. Sci.* 13, 347–350.
- (14) Poux, A. N., and Marmorstein, R. (2003) Molecular basis for Gcn5/PCAF histone acetyltransferase selectivity for histone and nonhistone substrates. *Biochemistry* 42, 14366–14374.
- (15) Thompson, P. R., Kurooka, H., Nakatani, Y., and Cole, P. A. (2001) Transcriptional coactivator protein p300 - Kinetic characterization of its histone acetyltransferase activity. *J. Biol. Chem.* 276, 33721–33729.



- (16) Liu, X., Wang, L., Zhao, K. H., Thompson, P. R., Hwang, Y., Marmorstein, R., and Cole, P. A. (2008) The structural basis of protein acetylation by the p300/CBP transcriptional coactivator. *Nature* **451**, 846–850.
- (17) Pal, S., Vishwanath, S. N., Erdjument-Bromage, H., Tempst, P., and Sif, S. (2004) Human SWI/SNF-associated PRMT5 methylates histone H3 arginine 8 and negatively regulates expression of ST7 and NM23 tumor suppressor genes. *Mol. Cell. Biol.* **24**, 9630–9645.
- (18) Cuthbert, G. L., Daujat, S., Snowden, A. W., Erdjument-Bromage, H., Hagiwara, T., Yamada, M., Schneider, R., Gregory, P. D., Tempst, P., Bannister, A. J., and Kouzarides, T. (2004) Histone deimination antagonizes arginine methylation. *Cell* **118**, 545–553.
- (19) Lieto, A. M., Lagerholm, B. C., and Thompson, N. L. (2003) Lateral diffusion from ligand dissociation and rebinding at surfaces. *Langmuir* **19**, 1782–1787.
- (20) Kim, Y., Tanner, K. G., and Denu, J. M. (2000) A continuous, nonradioactive assay for histone acetyltransferases. *Anal. Biochem.* **280**, 308–314.
- (21) Shogren-Knaak, M. A., and Peterson, C. L. (2004) Creating designer histones by native chemical ligation. *Methods Enzymol.* **375**, 62–76.
- (22) Smith, C. M., Gafken, P. R., Zhang, Z. L., Gottschling, D. E., Smith, J. B., and Smith, D. L. (2003) Mass spectrometric quantification of acetylation at specific lysines within the amino-terminal tail of histone H4. *Anal. Biochem.* **316**, 23–33.
- (23) Dyer, P. N., Edayathumangalam, R. S., White, C. L., Bao, Y. H., Chakravarthy, S., Muthurajan, U. M., and Luger, K. (2004) Reconstitution of nucleosome core particles from recombinant histones and DNA. *Methods Enzymol.* **375**, 23–44.
- (24) Clements, A., Rojas, J. R., Trievel, R. C., Wang, L., Berger, S. L., and Marmorstein, R. (1999) Crystal structure of the histone acetyltransferase domain of the human PCAF transcriptional regulator bound to coenzyme A. *EMBO J.* **18**, 3521–3532.
- (25) Clements, A., Poux, A. N., Lo, W. S., Pillus, L., Berger, S. L., and Marmorstein, R. (2003) Structural basis for histone and phosphohistone binding by the GCN5 histone acetyltransferase. *Mol. Cell* **12**, 461–473.
- (26) Lin, Y., Fletcher, C. M., Zhou, J., Allis, C. D., and Wagner, G. (1999) Solution structure of the catalytic domain of GCN5 histone acetyltransferase bound to coenzyme A. *Nature* **400**, 86–89.
- (27) Kuo, M. H., Zhou, J. X., Jambeck, P., Churchill, M. E. A., and Allis, C. D. (1998) Histone acetyltransferase activity of yeast Gcn5p is required for the activation of target genes in vivo. *Genes Dev.* **12**, 627–639.
- (28) Ma, J. C., and Dougherty, D. A. (1997) The cation- $\pi$  interaction. *Chem. Rev.* **97**, 1303–1324.
- (29) Taverna, S. D., Li, H., Ruthenburg, A. J., Allis, C. D., and Patel, D. J. (2007) How chromatin-binding modules interpret histone modifications: Lessons from professional pocket pickers. *Nat. Struct. Mol. Biol.* **14**, 1025–1040.
- (30) Yun, M. Y., Wu, J., Workman, J. L., and Li, B. (2011) Readers of histone modifications. *Cell Res.* **21**, 564–578.
- (31) Pesavento, J. J., Bullock, C. R., Leduc, R. D., Mizzen, C. A., and Kelleher, N. L. (2008) Combinatorial modification of human histone H4 quantitated by two-dimensional liquid chromatography coupled with top down mass spectrometry. *J. Biol. Chem.* **283**, 14927–14937.
- (32) Karmodiya, K., Krebs, A. R., Oulad-Abdelghani, M., Kimura, H., and Tora, L. (2012) H3K9 and H3K14 acetylation co-occur at many gene regulatory elements, while H3K14ac marks a subset of inactive inducible promoters in mouse embryonic stem cells. *BMC Genomics* **13**, No. 424.
- (33) Fraga, M. F., Ballestar, E., Villar-Garea, A., Boix-Chornet, M., Espada, J., Schotta, G., Bonaldi, T., Haydon, C., Ropero, S., Petrie, K., Iyer, N. G., Perez-Rosado, A., Calvo, E., Lopez, J. A., Cano, A., Calasanz, M. J., Colomer, D., Piris, M. A., Ahn, N., Imhof, A., Caldas, C., Jenuwein, T., and Esteller, M. (2005) Loss of acetylation at Lys16 and trimethylation at Lys20 of histone H4 is a common hallmark of human cancer. *Nat. Genet.* **37**, 391–400.
- (34) Zhu, P., Martin, E., Mengwasser, J., Schlag, P., Janssen, K. P., and Gottlicher, M. (2004) Induction of HDAC2 expression upon loss of APC in colorectal tumorigenesis. *Cancer Cell* **5**, 455–463.
- (35) Olsen, E. A., Kim, Y. H., Kuzel, T. M., Pacheco, T. R., Foss, F. M., Parker, S., Frankel, S. R., Chen, C., Ricker, J. L., Arduino, J. M., and Duvic, M. (2007) Phase IIB multicenter trial of vorinostat in patients with persistent, progressive, or treatment refractory cutaneous T-cell lymphoma. *J. Clin. Oncol.* **25**, 3109–3115.
- (36) Piekarczyk, R. L., Frye, R., Turner, M., Wright, J. J., Allen, S. L., Kirschbaum, M. H., Zain, J., Prince, H. M., Leonard, J. P., Geskin, L. J., Reeder, C., Joske, D., Figg, W. D., Gardner, E. R., Steinberg, S. M., Jaffe, E. S., Stetler-Stevenson, M., Lade, S., Fojo, A. T., and Bates, S. E. (2009) Phase II Multi-Institutional Trial of the Histone Deacetylase Inhibitor Romidepsin As Monotherapy for Patients With Cutaneous T-Cell Lymphoma. *J. Clin. Oncol.* **27**, 5410–5417.
- (37) Luger, K., Rechsteiner, T. J., and Richmond, T. J. (1999) Expression and purification of recombinant histones and nucleosome reconstitution. *Methods Mol. Biol. (Totowa, NJ, U. S.)* **119**, 1–16.
- (38) Shogren-Knaak, M. A., Fry, C. J., and Peterson, C. L. (2003) A native peptide ligation strategy for deciphering nucleosomal histone modifications. *J. Biol. Chem.* **278**, 15744–15748.
- (39) Ingenito, R., Bianchi, E., Fattori, D., and Pessi, A. (1999) Solid phase synthesis of peptide C-terminal thioesters by Fmoc/t-Bu chemistry. *J. Am. Chem. Soc.* **121**, 11369–11374.
- (40) Kent, S. (2010) Origin of the Chemical Ligation Concept for the Total Synthesis of Enzymes (Proteins). *Biopolymers* **94**, iv–ix.
- (41) Kent, S. B. H. (2009) Total chemical synthesis of proteins. *Chem. Soc. Rev.* **38**, 338–351.
- (42) Dawson, P. E., Churchill, M. J., Ghadiri, M. R., and Kent, S. B. H. (1997) Modulation of reactivity in native chemical ligation through the use of thiol additives. *J. Am. Chem. Soc.* **119**, 4325–4329.